

IDENTIFICATION OF TRANSFORMED GRAIN BOUNDARIES AND RECONSTRUCTION OF THE PRIOR GRAINS FROM EBSD DATA IN PURE Ti AND α -Ti ALLOYS

S.C. Wang¹, M.J. Starink², H.S. Ubhi³ and W.S. Li⁴

¹National Centre for Advanced Tribology, Engineering Sciences, University of Southampton, Southampton, SO17 1BJ, UK

²Materials Research Group, Engineering Sciences, University of Southampton, Southampton, SO17 1BJ, UK

³Oxford Instruments NanoAnalysis, High Wycombe, Bucks HP12 3SE, UK

⁴State Key Laboratory of Advanced Nonferrous Metal Materials, Lanzhou University of Technology, Lanzhou, 730050, China

Received: March 02, 2012

Abstract. When Ti is cooled rapidly from the β region, the $\beta \rightarrow \alpha$ martensitic transformation occurs. The transformed microstructure will be made up α phase grains, and the original structure of prior β grains is no longer evident from optical microscopy or electron microscopy. This paper demonstrates a simple way to well identify the transformation grain boundaries and accordingly reconstruct the prior grain structure through the use of electron backscattering diffraction on a scanning electron microscope. The approach is demonstrated for Ti and α -Ti alloy, and it is thought to be applicable to other alloys such as in iron, zirconium which have an orientation relationship between prior and formed grains.

1. INTRODUCTION

When Ti is cooled rapidly from above the β transus (882 °C for pure Ti), the α martensitic structure (or Widmanstätten) forms. The α plates and β matrix are oriented according to the so-called Burgers relationship:

$$\{1\bar{1}0\}_{\beta} // (0001)_{\alpha}, \quad \langle 111 \rangle_{\beta} // \langle 11\bar{2}0 \rangle_{\alpha}.$$

When two α laths with different variants adjoin in a prior β grain, a high angle grain boundary (HAGB, misorientation $> 10^\circ$) will be formed. For the Burgers orientation relationship there are 12 equivalent crystallographic variants. From a combination of any two of the 12 variants, there are 144 possible combinations which provide 6 crystallographically equivalent boundaries: one is a boundary with zero misorientation, i.e. identity and 5 are distinct types

of α/α HAGBs (Wang *et al.* 2003). These HAGBs are designated Types 2 to 6 and the reduced axis/angle pairs for each type are shown in Table 1.

Therefore, within a prior β grain, all the misorientations between α plates formed within the prior β grain belong to 5 types of α/α boundaries. On the boundaries between prior grains (β), the α/α boundary misorientations are essentially determined by the superposition of the original β/β misorientation angle and the 5 types of specific α/α boundaries. In general, these angles differ from the 5 types of specific α/α boundary orientations. As the original β/β misorientation angles were random, the α/α boundary angles at the location of the boundaries between prior grains will be random.

Measurements of grain boundaries or size between the variant of transformed phase are obtained effectively by electron backscattering diffraction

Corresponding author: S.C. Wang, e-mail address: wangs@soton.ac.uk

Table 1. The reduced axis/angle pairs for each type of α/α boundaries.

Type	Reduced axis/angle pairs
1	Identity
2	$\langle 11 \bar{2} 0 \rangle / 60^\circ$
3	$\langle 1.377, -2.377, 1, 0.359 \rangle / 60.83^\circ$
4	$\langle 55 \bar{1} \bar{0} \bar{3} \rangle / 63.26^\circ$
5	$\langle 1.377, -2.377, 1, 0 \rangle / 90^\circ$
6	$\langle 0001 \rangle / 10.53^\circ$

(EBSD) in scanning electron microscopy (SEM). But this type of EBSD data does not directly provide the grain size of the prior phase (β phase in case of Ti). The previous study (Germain *et al.* 2005) in the near alpha titanium alloy (IMI834 developed specifically for service in high pressure compressors of aero gas turbine engines) showed the fatigue resistance largely depends on the local textures of macrozones (i.e. the prior β phase). Gey and Humbert (2003) had derived an orientation map of the parent β phase from that of the α inherited phase, but they could not identify all the α inherited orientations. The identification of every type of α/α boundaries is equally important as it is crucial in analysing the texture evolution and therefore alloy stability. For example, in tensile test on IMI834, the crack planes were initiated from the (0001) (Bache *et al.* 1997), which is Type 6 as shown in Table 1. Therefore, it is essential to have knowledge of all types of α grain boundaries. This paper demonstrates a simple way to identify the transformation grain boundaries and reconstruct the prior grains. In the present approach we will identify the observed HAGB angles and compare to those predicted by martensitic transformation theory (see e.g. (Wang *et al.* 2003)). The method will be demonstrated for in a pure Ti and a Ti-6Al-4V alloy.

2. EXPERIMENTAL PROCEDURE

All experiments were performed on commercial purity grade Ti and on a Ti-6Al-4V alloy. The latter is one of most common Ti alloys. The specimens were solution treated at 1000 °C followed by a quench into water to produce a microstructure consisting of a fine distribution of α laths. The specimen for EBSD was ground using SiC papers starting from 180 grit and ending at 1200 grit and subsequently electro-polished using a solution of 33% HNO₃ and 67% methanol at a temperature of -20-30 °C. Orientation measurements were taken in the JEOL FEG-SEM 6500F using an automated EBSD system (Channel 5 software from HKL, Denmark). Step sizes were chosen as 0.5 μ m and 2.5 μ m for small and larger areas, respectively.

3. APPLICATION

Fig. 1a shows the EBSD band contrast (BC) map of α/α grain boundaries in a relatively small area for the pure Ti alloy. The contrast map reveals the EBSD quality, which in this case is good. The corresponding misorientation angle distributions (Fig. 1b) reveal four peaks located around 10°, 60°, 63°, and 90°, which are consistent with the expected α/α boundaries in this system as shown in Table 1, i.e., misorientation angle distributions correspond to Type 6, Types 2 and 3, Type 4 and Type 5, respectively. Analysis of the EBSD data showed that this area contains 486 α/α HAGBs. We can identify the different type of α/α boundaries in Fig. 1a using the EBSD software. In the HKL 5 software used here, the identification of grain boundaries with specific indices/angle can be used either in the Miller system (3 index coordinates) or Miller-Bravais indices (4 index coordinates), but index numbers may be limited to maximum integers less than 10. Therefore, we need to simplify the axis indices in Table 1 to the axes in integers, which are close to axes in fractions and the integers are less than 10, in either

Table 2. The reduced axis/angle pairs for each type of α/α boundaries.

Type	Reduced axis/angle pairs(3 index system)	Deviation of integer axes away from ones in Table 1
2	[110] / 60°	0°
3	[1 $\bar{9}$ 1] / 60.83°	0.48°
4	[551] / 63.26°	0°
5	[1 $\bar{9}$ 0] / 90°	0.02°
6	[001] / 10.53°	0°

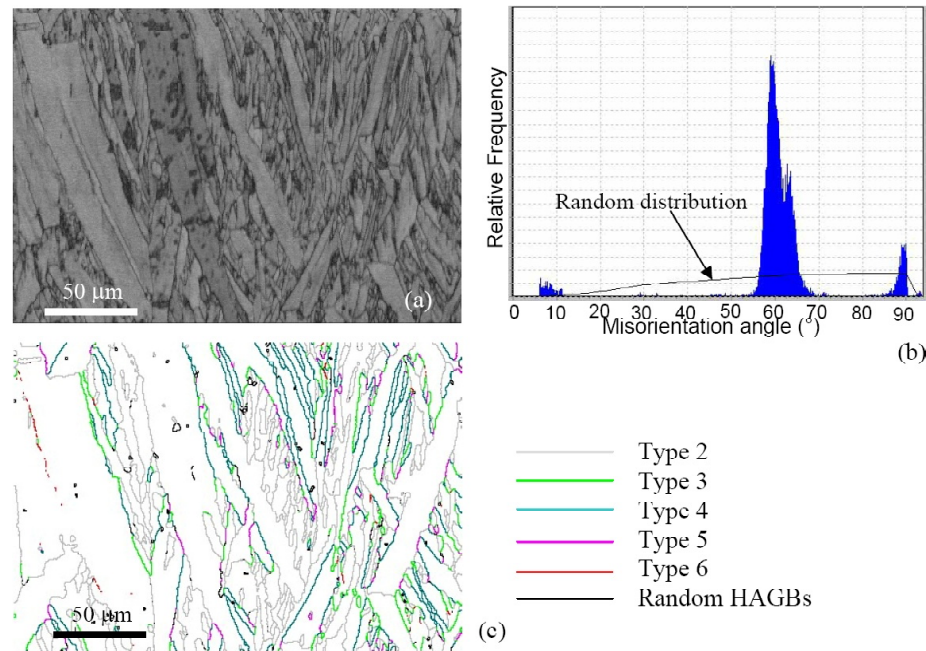


Fig. 1. (a) Band contrast map revealing the EBSD quality in a small area of pure Ti. (b) The corresponding frequency distribution against misorientation angle. The black line represents the theoretical random distribution of misorientation angles. (c) The grain boundary map revealing the different types of alpha variants in the same region as Fig. 1a.

4 or 3 index system (The procedure may need to be repeated to find the best fit.) In the case of α/α boundaries, the nearest axis of integer indices are shown in Table 2 (in the Miller system).

Accordingly all types of alpha variants can be clearly distinguished, and can be presented for instance using different colours in colour micrographs as shown in Fig. 1c. Of the HAGBs weighted by boundary length, 55.5% is Type 2, 12.8% is Type 3, 25.6% is Type 4, 5.2% is Type 5 and 0.8% is Type 6. The relative amounts can be compared with a theory in Wang *et al.* (2003) in which two types of nucleation events are considered: stochastic nucleation wherein the probability of forming any one of the 12 orientation variants is equal, and sympathetic nucleation of the variant required to complete a self-accommodating three-variant cluster of the type described in (Wang *et al.* 2003). The measured relative amounts are broadly in agreement with theoretical predictions in Wang *et al.* (2003), providing support that the present interpretation of the origin of the grain boundaries is correct. Specifically the strong preference for the formation of Types 2 and 4 variants (totalling 74% in the model predictions and measured here at 81%) is due to the self-accommodation on the α/α boundaries; the low amount of Type 5 boundaries and near absence of Type 6 boundaries is also in line with theory (Wang *et al.* 2003).

Fig. 2a shows the α/α grain boundary BC map for a relatively large area ($1240 \times 930 \mu\text{m}^2$) with 4229 α/α HAGBs. Boundaries of prior grains (β) cannot be discerned from such a map. Fig. 2b shows the corresponding frequency-misorientation angle distributions. Compared to Fig. 1b, two extra peaks exist: one at 30° and another at $\sim 94^\circ$. As they do not belong to any of the α/α grain boundaries types obtained by the Burgers transformation, these extra peaks must be caused by superposition of boundary angles of the prior β grains with the 5 specific α/α type boundary angles. If we exclude the peaks around 30° and 94° , the frequencies of HAGBs (weighted by boundary length) are 57.9% Type 2, 13.3% Type 3, 23.6% Type 4, 4.5% Type 5 and 0.7% Type 6. All Types 2-6 of alpha variants can be clearly distinguished, and can be presented using lines in different colours in the same manner as shown in Fig. 1c. The α/α boundaries which do not belong to Types 2-6 are drawn in black lines as shown in Fig. 3c. These grain boundaries drawn in black and white of the results is obtained by superimposing the Types 2-6 boundaries in white and the other HAGB in black onto the band contrast map. The result in Fig. 2d shows substantial detail of the grain structure with the prior β grain boundaries accentuated by the dark lines.

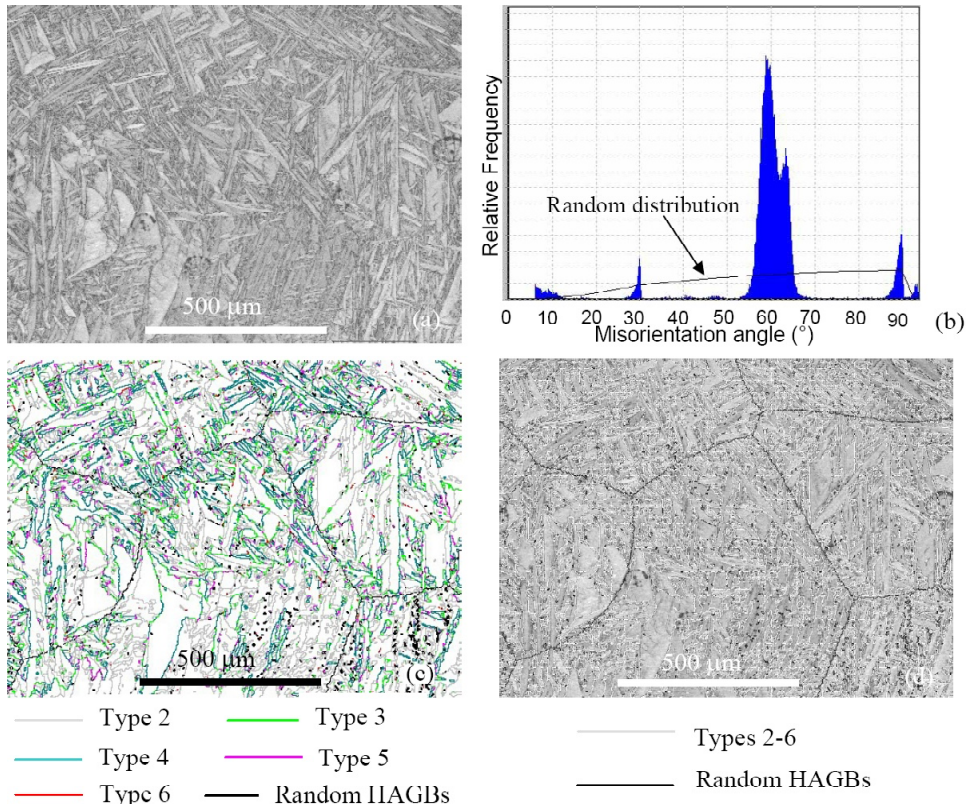


Fig. 2. (a) Band contrast map in a large area of pure Ti. (b) The corresponding frequency distribution against misorientation angle. (c) The grain boundary map revealing the different types of alpha variants in the same region as Fig. 2a; (d) The grain boundary and band contrast maps revealing the boundary map of prior β phase in the same region to Fig. 2a. The silver and dark lines represent boundaries of Types 2-6 and random misorientations, respectively.

The same treatment is applied to the Ti6Al4V alloy. Fig. 3a shows the α/α grain boundary BC map for a large area. Fig. 3b shows the corresponding frequency-misorientation angle distributions. Fig. 3c shows the EBSD map with all Types 2-6 of α/α boundaries presented in different colours. In this alloy the α grains are much smaller as compared to the pure Ti alloy. The frequencies of HAGBs are determined to be 20.2% Type 2, 23.6% Type 3, 44.1% Type 4, 1.7% Type 5, and 10.4% Type 6. These relative amounts are not quite in line with the theoretical predictions based on two types of nucleation events: stochastic nucleation wherein the probability of forming any one of the 12 orientation variants is equal, and sympathetic nucleation of the variant required to complete a self-accommodating three-variant cluster. However, the amount of Type 6 boundaries is about 3 times higher as theory predicts, whilst the combined amount of Type 2 and 4 boundaries is lower than these predictions. This difference might suggest that in the ternary alloy the influence of self-accommodation as a driving force for selecting orientations is much reduced as

compared to the pure Ti. Using the same procedure as used in Fig 2d, a map with the Types 2-6 boundaries in white and the other HAGB in black superimposed onto the band contrast map is obtained. The result in Fig. 3d shows substantial detail of the grain structure with the prior α grain boundaries accentuated by the dark lines.

Solid state phase transformations in which the whole of the parent phase is consumed on cooling are very common in a wide range of alloys. For example, in steel, the face-centred cubic (f.c.c) austenite phase (γ) will transform to body-centred cubic (b.c.c) ferrite (α) when the temperature is lower than ~ 830 °C, and in many steels the austenite can be completely consumed. Martensitic transformations will occur by rapid cooling such as water quench. According to different alloying compositions, a variable orientation relationships may exist, such as the Kurdjumov-Sachs (K-S) relation (1930) ($\{111\}_{\gamma} // (011)_{\alpha}, < \bar{1} 01 >_{\gamma} // < \bar{1} \bar{1} 1 >_{\alpha}$) in Fe-1.4 wt.% C, the Nishiyama relation (Nishiyama 1978) ($\{111\}_{\gamma} // (011)_{\alpha}, < \bar{1} \bar{1} 2 >_{\gamma} // < 0 \bar{1} 1 >_{\alpha}$) in Fe-30 wt.% Ni, and the Pitsch relation (Pitsch 1962)

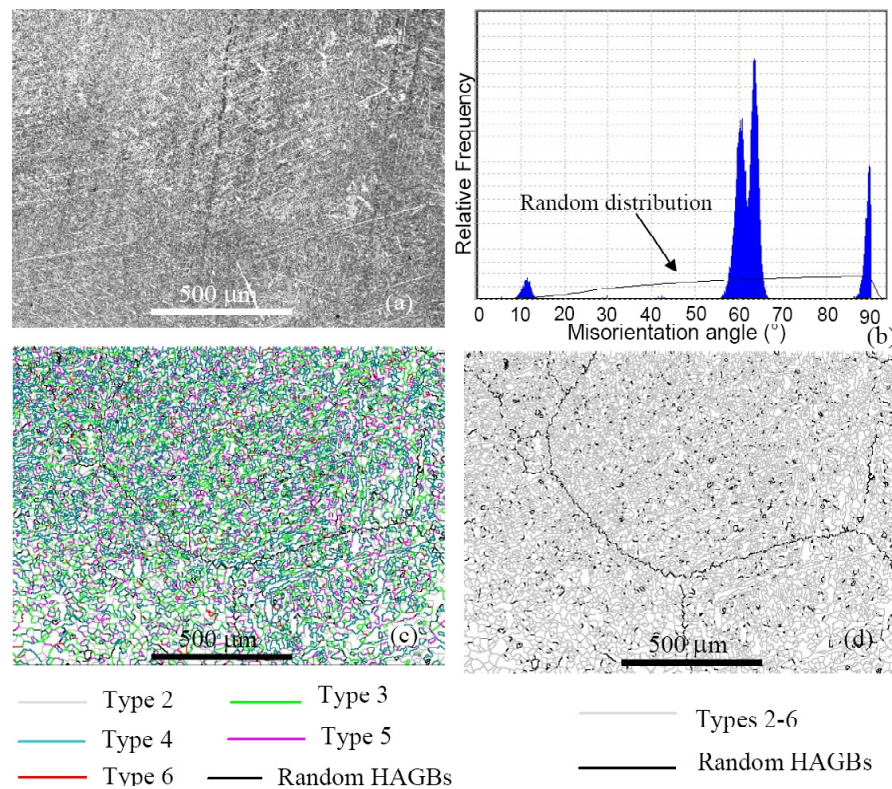


Fig. 3. (a) Band contrast map in a region of Ti6Al4V alloy. (b) The corresponding frequency distribution against misorientation angle. (c) The grain boundary map revealing the different types of alpha variants in the same region as Fig. 3a. (d) The grain boundary and band contrast maps revealing the boundary map of prior β phase in the same region to Fig. 3a. The silver and dark lines represent boundaries of Types 2-6 and random misorientations, respectively.

$(\{101\}_{\gamma} // (112)_{\alpha}, < \bar{1}01 >_{\gamma} // < \bar{1} \bar{1} 1 >_{\alpha})$ in Fe-1 wt.% C, Fe-1.5 wt.% N and Fe-29 wt.% Ni. Because the transformation product (α in steel) adopts a specific orientation relationship with respect to the prior parent grain (γ in steel), the number of product variants that can be formed in such a grain is fixed, i.e. only a limited number of relative orientations between adjacent variants can be produced. It is thought that the same procedure can be applied to these martensite transformation reactions through distinguishing the transformed and random orientations.

5. CONCLUSIONS

This paper demonstrates a simple way to reconstruct the prior grain by distinguishing the 5 types of α/α boundaries using EBSD. The method uses the fact that Martensite transformation leads to formation of specific and random orientations. The specific orientations are formed due to the transformation product adopting a specific orientation relationship with respect to the prior parent grain. The random orientations are formed

on the boundaries between prior grains (β). Thus the prior grain structure can be reconstructed by excluding the 5 types of α/α boundary misorientations from EBSD measurements of grain boundary misorientations.

REFERENCES

- [1] S.C. Wang, M. Aindow and M.J. Starink // *Acta Mater.* **51** (2003) 2485.
- [2] L. Germain, N. Gey, M. Humbert, P. Bocherand and M. Jahazi // *Acta Mater.* **53** (2005) 3535.
- [3] N. Gey and M. Humbert // *J. Mat. Sci.* **38** (2003) 1289.
- [4] M.R. Bache, M. Cope, H.M. Davies, W.J. Evans and G. Harrison // *Int. J. Fatigue* **19** (1997) S83.
- [5] G.V. Kurdjumov and G. Sachs // *Z. Phys.* **64** (1930) S325–43.
- [6] Z. Nishiyama, *Martensitic Transformation* (Academic Press, New York, 1978).
- [7] W. Pitsch // *Acta Metall.* **10** (1962) 897.